Evaluating the snow component of a flood forecasting model

T. Nester, R. Kirnbauer, J. Parajka and G. Blöschl

ABSTRACT

The objective of this study is to evaluate the snow routine of a semi-distributed conceptual water balance model calibrated to streamflow data alone. The model is used for operational flood forecasting in 57 catchments in Austria and southern Germany with elevations ranging 200–3,800 m a.s.l. We compared snow water equivalents (SWE) simulated by the hydrologic model with snow covered area (SCA) derived from a combined product of MODIS (version 5) Terra and Aqua satellite data for the period 2003–2009 using efficiency measures and a spatial analysis. In the comparison, thresholds for percent catchment snow cover and a cut-off water equivalent need to be chosen with care as they affect the snow model efficiency. Results indicate that the model has a tendency to underestimate snow cover in prealpine areas and forested areas while it performs better in alpine catchments and open land. The spatial analysis shows that for 88% of the analysed model area snow cover is modelled correctly on more than 80% of the days. The space borne snow cover data proved to be very useful for evaluating the snow model. We therefore suggest that the snow data will be similarly useful for data assimilation in real time flood forecasting.

Key words | flood forecasting, model validation, MODIS snow cover

T. Nester (corresponding author)
R. Kirnbauer
J. Parajka
G. Blöschl
Institute of Hydraulic Engineering and Water Resources Management,
Vienna University of Technology,
Vienna,
Austria
E-mail: *nester@hydro.tuwien.ac.at*

INTRODUCTION

Recent flood events in Austria such as the 2002 flood in the Danube basin have raised the public awareness for the need for flood warnings to reduce damage to property and life. Following these floods, operational flood forecasting systems have been developed for most rivers in Austria. These include the Kamp River (Blöschl *et al.* 2008), the Inn River (Kirnbauer & Schönlaub 2006), and the Mur River (Schatzl & Ruch 2006).

The challenge of operational forecasting systems is the need for simple and robust, yet accurate, routines that can be used with a limited amount of real time data. The forecasting is, thus, particularly difficult in mountainous regions because of the large spatial variability of hydrologic characteristics and the limited availability of ground based hydrologic data. As the prediction of streamflow depends on the accuracy of input data and the state variables of the model, it is important to estimate state variables such as soil moisture and snow water equivalent (SWE) well. Recent studies suggest that remote sensing data may be valuable for validating the snow component of hydrological models and assimilating them into forecast models.

To evaluate snow models, different remote sensing products have been used, especially in alpine regions where forests do not obstruct the detection of snow. Blöschl & Kirnbauer (1992) obtained snow cover patterns from aerial photographs and used them to validate a snow model (Blöschl *et al.* 1991). From the differences between simulated and observed patterns they evaluated the effects of radiation and wind transport on the snow distribution. Blöschl *et al.* (2002) used SPOT XS satellite data to reduce the biases in simulated SWE. Garen & Marks (2005) found good agreement between the temporal evolution of simulated and satellite snow covered area (SCA) for three snowmelt seasons in a basin in Idaho, but they also found that the satellite data underestimated SCA in forested areas. Koboltschnig *et al.* (2008) used LANDSAT TM and

doi: 10.2166/nh.2012.041

ASTER L1B data to compare simulated and SCA in a glaciated catchment in the Austrian Alps. Results showed that the model overestimated the observation by 1–9% in June and July and by 10–36% in August and September which they attributed to redistribution of snow by wind or avalanches not included in the model. Schöber *et al.* (2010) used LANDSAT images to evaluate SCA simulations in glaciated catchments in Tyrol and showed an average model underestimation of 17%. Studies in non-alpine areas include Wigmosta *et al.* (1994), who used NOAA-AVHRR SCA to validate simulated snow cover patterns in Montana. Roy *et al.* (2010) compared MODIS SCA to *in situ* snow depth measurements and simulated SCA in a forested study region in Canada. They developed a direct-insertion approach defining an empirical threshold for SWE to compensate for discrepancies between modelled SWE and satellite derived SCA. Zappa (2008) assessed the performance of distributed snow cover simulations in Switzerland, adopting skill scores based on contingency tables for a quantitative evaluation of snow cover simulations and comparing NOAA-AVHRR snow cover data to the model results. He showed that the model captures the observed patterns with high accuracy and that the scores allow an objective quantification of such agreement. However, the results of Zappa (2008) reveal that the largest uncertainties are present in the regions of the transition zones between the valley plains and the upper part of the valley slopes.

MODIS snow cover data (SCA) are appealing for regional scale modelling and validation. The main advantage of MODIS imagery is the high temporal and spatial resolution and mapping accuracy. Comparisons of MODIS snow cover data with other satellite products and ground based snow depth measurements showed mapping accuracy between 90 and 95% in cloud free conditions, but varying with land cover, snow conditions and snow depth (see e.g., Klein & Barnett 2003; Simic *et al.* 2004; Tekeli *et al.* 2005; Parajka & Blöschl 2006; Hall & Riggs 2007; Pu *et al.* 2007; Tong *et al.* 2009b; Parajka & Blöschl 2012). The main limitation, however, is persistent cloud coverage, which can significantly limit MODIS application for snow cover mapping and its usefulness for assimilation into hydrologic models (e.g., Rodell & Houser 2004; Parajka & Blöschl 2008b; Şorman *et al.* 2009; Tong *et al.* 2009a). Different methods to reduce cloud coverage have been developed (see e.g., Parajka & Blöschl 2008a; Gafurov & Bárdossy 2009; Tong *et al.* 2009b; Hall *et al.* 2010; Parajka *et al.* 2010). Parajka & Blöschl (2006) show that MODIS classification errors are around 15% in the winter months and around 1% in summer; however, this is related to the larger spatial extent of clouds in the winter months. On average, Parajka & Blöschl (2006) have estimated a spatial extent of clouds over Austria of 63% for the years 2000–2005. Recently, MODIS SCA data have been assimilated into hydrological models (see e.g., Andreadis & Lettenmaier 2006; Roy *et al.* 2010; Thirel *et al.* 2011) and used for model calibration (see e.g., Déry *et al.* 2005; Tekeli *et al.* 2005; Udnaes *et al.* 2007; Parajka & Blöschl 2008b; Immerzeel *et al.* 2009; Şorman *et al.* 2009), mostly indicating that using MODIS data improves the snow simulations more than it does the streamflow simulations.

In most of the basins in the present study, springtime streamflow is highly influenced by the water stored in the snow pack. Especially for flood forecasting it is vital to estimate the available water storage as accurately as possible. As highlighted in the literature, using MODIS snow cover data show much promise for model evaluation. However, most studies evaluated the snow models over a short time period because prevailing cloud cover limited the available remote sensing data. Thus, the objective of the present study is (1) to investigate whether MODIS data with a large spatial extent of cloud coverage over a basin can be used for evaluating a snow model, (2) to examine the evaluation method in terms of the thresholds used, and (3) to analyse the temporal and spatial performance of the snow component of an operational flood forecasting model using observed SCA data derived from MODIS. We use a semi-distributed conceptual hydrological model in a simulation mode with historical data and MODIS data version 5 (Riggs *et al.* 2006) from 2003–2009 as an independent data set.

The paper is organised as follows. The data section gives details on the study area and the ground and satellite data used in the paper. The Methods section gives a short description of the calibration of the model and the error measures used to evaluate the snow model performance. In the Results section, a sensitivity analysis to evaluate threshold values on the snow model performance is carried out and the errors are analysed in regard to seasonality and elevation; the model performance is evaluated in space and

time. The final section discusses the results and concludes with remarks on potential future applications of remote sensing snow cover data in operational flood forecasting. In Appendix A (available online at http://www.iwaponline.com/nh/043/041.pdf), a description of the model is given.

STUDY REGION AND DATA

The flood forecasting system for the Austrian Danube consists of three parts: (1) a meteorological, (2) a hydrological and (3) a hydraulic model part. The meteorological forecasts include deterministic and ensemble forecasts of precipitation and air temperature for 48 hours on an hourly time step; the hydrological model estimates deterministic and ensemble streamflow forecasts in the Danube tributaries; and the hydraulic model is run with the results from the hydrological model to estimate streamflow and water level for the Danube River. In this study, we focus on the evaluation of the snow model. For this purpose we ran the hydrological model with observed meteorological data. The study region includes the tributaries to the Danube River which cover a large part of Austria and some parts of Bavaria. Hydrological conditions are quite diverse. In the alpine west elevations range up to 3,800 m a.s.l. while the north and east consist of prealpine terrain and lowlands with elevations between 200 and 800 m a.s.l. (Figure 1). Land use is mainly agricultural in the lowlands, forests in the medium elevation ranges and alpine vegetation, rocks and glaciers in the alpine catchments. The alpine catchments are generally wetter with mean annual precipitation of almost 2,000 mm yr^{-1} in the west compared to 600 mm yr^{-1} in the east.

The hydrologic data set used in this study includes hourly streamflow data of 57 gauged and telemetered catchments with sizes ranging from 70 to 25,600 km to calibrate and validate the model. The data set also includes hourly values of precipitation, air temperature and potential evapotranspiration. Precipitation and temperature measurements for the years 2003 to 2009 were spatially interpolated by the Central Institute for Meteorology and Geodynamics (ZAMG) in Vienna using the algorithm implemented in the INCA system (Steinheimer & Haiden 2007; Haiden & Pistotnik 2009). The INCA system was developed by the ZAMG mainly for meteorological forecasting, but it can also be used with historical data. INCA uses output from surface station observations, radar data and elevation data to generate gridded weather data. For the precipitation analysis, a combination of interpolated station data including elevation effects and spatially structured radar is used. The procedure of combining the different data is given in Haiden *et al.* (2010). The spatial distribution of potential

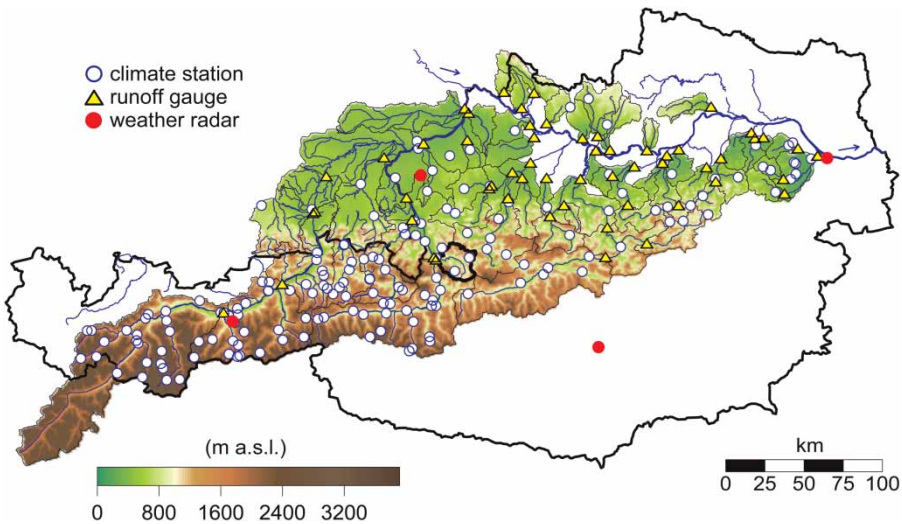

Figure 1 | Topography of Austria and parts of southern Germany. The stream gauges used in the study are indicated by triangles, precipitation gauges by white circles, weather radar stations by red circles. Thin black lines are catchment boundaries, the thick black line highlights the catchment Obergäu/Lammer used for detailed analyses. The colour version of this figure is available in the online version of the paper (http://www.iwaponline.com/nh/toc.htm).

evapotranspiration was estimated from hourly temperature and daily potential sunshine duration by a modified Blaney-Criddle equation (DVWK 1996). This method has been shown to give plausible results in Austria (Parajka *et al.* 2003). To calibrate and verify the model on streamflow data, the years 2003–2006 were used as calibration period; 2007–2009 were used as a validation period.

Once the hydrologic model was calibrated and in operational use, we were interested in how the model fits to the MODIS data which are an independent source of information as they were never used for calibration. The MODIS data used for evaluating the snow routine are based on daily observations acquired by the Terra and Aqua satellites of the NASA Earth Observation System. We used the approach of Parajka & Blöschl (2008a) to merge the original Version 5 Terra (MOD10A1) and Aqua (MYD10A1) MODIS products (Hall *et al.* 2006, 2007) in space and time on a pixel basis. The MODIS snow cover maps were reclassified from originally 16 pixel classes to three categories: snow, no snow (land) and clouds. The snow class was retained as snow. The snow free land class was retained as no snow (land). The cloud, missing and erroneous data classes were combined into clouds. However, missing and erroneous data represent only a small portion of the total data. The remaining 11 original classes did not occur in the computations of this study. Based on the following assumptions, four pixels with the size of 500×500 m were aggregated to obtain snow cover maps with a pixel size of 1×1 km: (1) if all four pixels were marked as the same category, the category of the 1×1 km pixel remained the same, (2) if the number of pixels marked as no snow was greater than the number of snow pixels, the 1×1 km pixel was classified as no snow, and (3) if the number of pixels marked as snow was greater or equal than the number of pixels marked as no snow, the 1×1 km pixel was classified as snow.

The average cloud cover over the study region for the period 2003–2009 (total of 2,555 days) is around 50% for the combined Aqua-Terra-MODIS data. Cloud coverage is around 40% in alpine valleys and around 60% over mountainous terrain. Figure 2 (top) shows the spatial distribution of the cloud coverage for the period 2003–2009 in the model region. Figure 2 (bottom) shows the long-term ratio of snow covered days (*SCD*) for 2003–2009. For every pixel, the ratio of snow covered days (S_{MODIS}) to snow covered plus snow free days (L_{MODIS}) was determined; days with cloud cover were not considered. As expected, the ratio of *SCD* closely follows the elevation in the area: in the alpine region the percentage of snow covered days is much higher than in the lowlands in the east and north of the Alps. Similarly, the alpine valleys show a smaller percentage of snow covered days than the higher elevations. The mean snow cover in the model region is 30% for cloud free days for 2003–2009.

METHODS

Model structure and calibration

The rainfall runoff model used in this study is a conceptual hydrological model which is applied in a semi-distributed mode. The model is operationally used for flood forecasting for the Austrian Danube tributaries; in this study, however, we use the model in a simulation mode with historical data. The structure is similar to that of the HBV model (Bergström 1976). Detailed information about the model structure is given in Appendix A and in Blöschl *et al.* (2008). Parameters were estimated manually and separately for each of the 57 catchments for the entire calibration period 2003–2006. First, nested catchments were calibrated. Parameter values of these basins were then considered to be constant and the remaining parts of the catchment were calibrated. The calibration process followed a number of steps (Blöschl 2008). The first step was an approximation of the annual water balance. As snow is a major component of the water balance in the study area and can influence the soil moisture state throughout the year, initial parameters for the slow flow components, for the maximum soil moisture storage and the snow routine were set in this first step. Then, the initial model parameters were adjusted in order to reproduce seasonal patterns correctly. Threshold temperatures were adjusted, as well as parameters influencing the slow components. The last step was to parameterise the fast flow components and the parameters of the linear storage cascade by looking at single flood events as well as a fine tuning of the parameters of the snow and soil moisture routines. The main goal of the calibration was to estimate the timing of the rising limbs and the peak discharge as

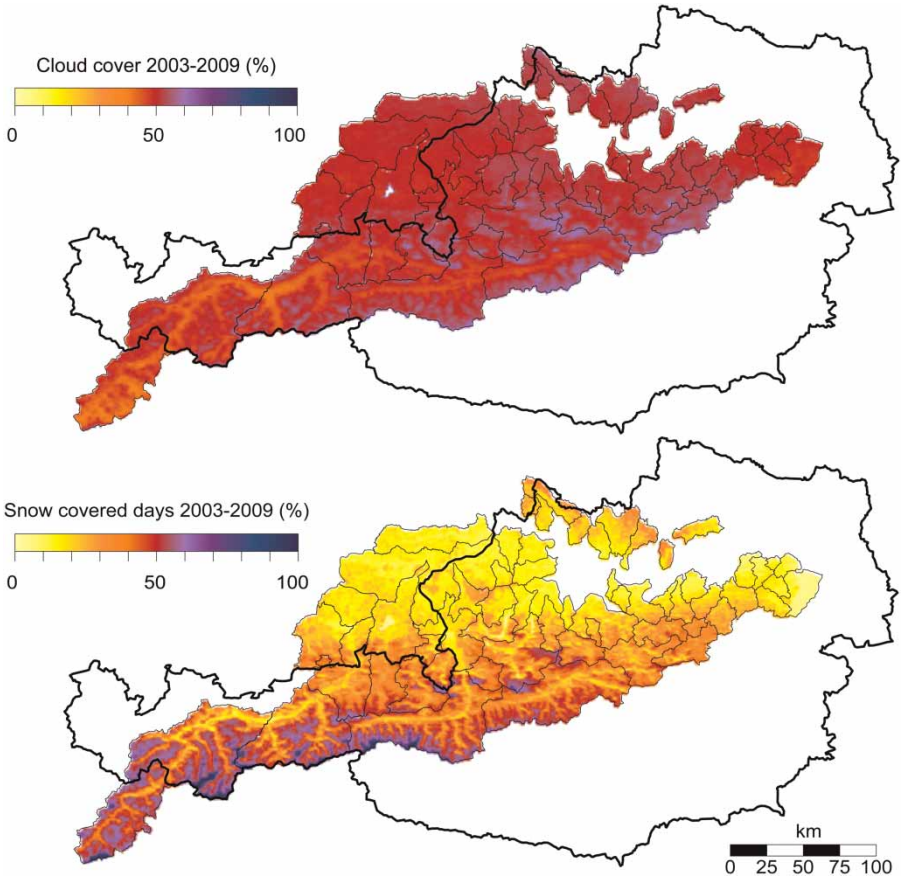

Figure 2 | Top: cloud cover for the years 2003 to 2009 in the model region. Average cloud cover for the months October to May is 50%. Bottom: long-term ratio of snow covered days (S_{MODIS}) to snow covered plus snow free days (L_{MODIS}) for the years 2003 to 2009, according to MODIS. The thick black line indicates Austria; thin black lines indicate the model areas. White indicates no data and area outside the model region. A colour version of this figure is available in the online version of the paper (http://www.iwaponline.com/nh/toc.htm).

well as the magnitude of the peak discharge as correctly as possible. After each model run, we visualised the model simulations and evaluated the results using statistical measures for the entire calibration period.

For the calibration of the snow routine, the snow correction factor C_S was set to a value of 1, as an elevation-based correction of precipitation is part of the INCA system (Haiden & Pistotnik 2009). The choice of threshold temperatures was guided by Seibert (1999) who used values ranging from −1.5 to 2.5 °C and a degree day factor ranging from 1 to 10 mm °C^{-1} day^{-1} for his Monte Carlo based calibration in Sweden. Braun (1985) used a temperature range from −2.0 to 4.0 °C in lowland and lower-alpine catchments in Switzerland where a mix of rain and snow can occur, whereas Kienzle (2008) proposed wider threshold temperatures range from $T_s = -4$ °C to $T_r = 8$ °C for Canada. Merz *et al.* (2009) preset values of 0 and 2 °C for the threshold temperatures T_s and T_r, respectively, and produced accurate streamflow simulations at the daily time scale. We estimated parameters for T_s from −1.8 to −0.4 °C and for T_r in the range 0.8 to 1.6 °C in our model area. The threshold temperatures are well in the range of other studies. The remaining parameters of the snow routine are in the range of the parameters in Merz & Blöschl (2004), who estimated the parameters with an automatic algorithm. The melt temperature T_m was set to values in the order of 0.1–0.9 °C; the degree day factor D is in the range 1.3–2.3 mm °C^{-1} day^{-1} and doubles during rain-on-snow events (Sui & Koehler 2001). Table 1 gives an overview of the range of the calibrated snow routine model parameters; additional details on the calibration are given in Nester *et al.* (2011).

Table 1 | Hydrologic model parameters of the snow routine

Model parameter	Description	Min in region	Max in region
D	Degree day factor (mm.°C^{-1}.day^{-1})	1.3	2.3
T_s	Threshold temperature (°C)	−1.8	−0.4
T_r	Threshold temperature (°C)	0.8	1.6
T_m	Melt temperature (°C)	0.1	0.9
C_S	Snow correction factor (–)	1.0	1.0

Figure 3 shows the model results for the winter months (October to May) for the gauge Obergäu/Lammer (catchment highlighted in Figure 1). The gauge is shown as a representative example for an alpine catchment with elevations ranging from 470 to 2,400 m a.s.l. Ten percent of the catchment area is below 750 m a.s.l., 50% of the area is between 750 and 1,250 m a.s.l., 30% is between 1,250 and 1,750 m a.s.l. and the remaining 10% of the catchment area is at elevations higher than 1,750 m a.s.l. The top panels refer to the calibration period of the

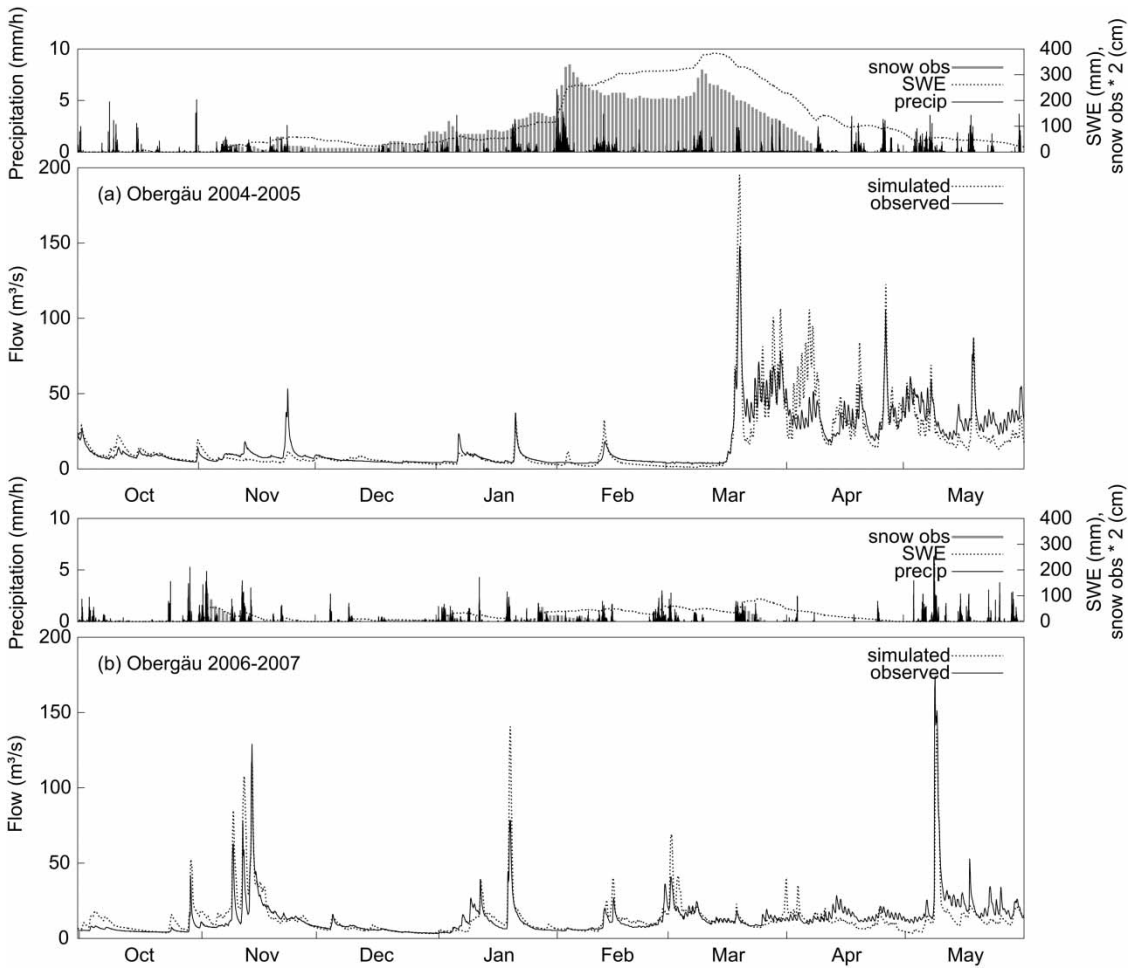

Figure 3 | Observed and simulated hydrographs for the winter seasons 2004–2005 (calibration period of the hydrological model – top) and 2006–2007 (validation period of the hydrological model – bottom) for the gauge Obergäu/Lammer. Snow depth measurements for a single station (Annaberg, 700 m a.s.l.) in the catchment are shown.

hydrological model and show the winter season 2004–2005. Starting at the end of October, most of the precipitation is accumulating as snow, and only a small amount of precipitation is directly contributing to runoff. For comparison of the snow model results we plotted modelled basin average SWE values and observed snow depths of the only station in the catchment where snow data were available (elevation 700 m a.s.l.). The peaks in the winter season are simulated well. At the beginning of March, the modelled SWE is close to 400 mm; snow melt starts at the middle of the month. The timing of the rise is simulated well but the peak is overestimated. Until mid April, the model is overestimating the snow melt induced streamflow but the daily characteristics of the snow melt is reproduced well. Several storm events increase the runoff rapidly. The lower panels refer to the validation period of the model, showing the winter season 2006–2007. In this winter, less snow has been accumulated to a maximum SWE of around 100 mm. Several short storms directly contribute to the runoff or in a combination of melt and rain, e.g., in November and in January. Again, the snow melt starts in the middle of March but in this year the snow melt period is underestimated by the model. We used different statistical measures to evaluate the performance of the model including the Nash & Sutcliffe (1970) coefficient of efficiency (*nsme*):

$$nsme = 1 - \frac{\sum_{i=1}^{n}\left(Q_{\mathrm{sim},i} - Q_{\mathrm{obs},i}\right)^2}{\sum_{i=1}^{n}\left(Q_{\mathrm{obs},i} - \overline{Q_{\mathrm{obs}}}\right)^2}, \quad (1)$$

where $Q_{\mathrm{obs},i}$ and $Q_{\mathrm{sim},i}$ are observed and simulated runoff at hour i, respectively, and $\overline{Q_{\mathrm{obs}}}$ is the mean observed runoff over the calibration or validation period of n hours. *nsme* values can range from $-\infty$ to 1. A perfect match between simulation and observation implies $nsme = 1$; $nsme = 0$ indicates that the model predictions are as accurate as the mean of the observed data, and $nsme < 0$ occurs when the observed mean is a better predictor than the model. For the entire calibration period (summer and winter) the *nsme* for the gauge Obergäu/Lammer is 0.60, for the validation period it is 0.69. For the periods shown in Figure 3, *nsme* is 0.69 for the winter 2004–2005 and 0.65 for the winter 2006–2007. Details on the model performance are given in Nester *et al.* (2011).

For the evaluation of the snow model, we had to consider that the model results are available on an hourly time step whereas MODIS data are available on a daily basis. Typically, Aqua data are acquired around 1 p.m. and Terra data around 11 a.m. over Austrian territory. Therefore we used the model results at 12 noon for the evaluation. Also the model simulates uniform SWE within each elevation zone of a catchment, which can be considered either snow covered or snow free, depending on a threshold value chosen. Threshold values for snow depth used in the literature include 2 cm (Tong *et al.* 2009b), 2.5 cm (Tekeli *et al.* 2005), 3.5 cm (Klein & Barnett 2003) and 4 cm (Roy *et al.* 2010). As a starting point, we considered simulated SWE larger than the threshold $\xi_{\mathrm{SWE}} = 2.5$ mm as snow covered. In Figure 4 the same periods as in Figure 3 are plotted in order to evaluate the temporal evolution of the SCA. The top panels show the mean hourly catchment temperature in the range from -10 to 10 °C. The lower panels show basin average SCA derived from both MODIS and the model results. MODIS SCA values are shown as circles in different sizes, the size of the markers referring to the different cloud coverage classes. Large circles denote days with cloud coverage less than 50%, when MODIS data contain a great deal of information. Medium sized circles indicate less information about the snow extent (cloud coverage ranging from 50 to 80%). Small circles relate to cloud coverages ranging from 80 to 95%. Hourly model-based SCA values were calculated only from cloud free pixels for consistency of catchment area. Both figures indicate that the timing of the snow accumulation is accurately simulated. The modelled SCA values increase at the same time as the MODIS SCA. Similarly, the timing of the beginning of the snow depletion between simulation and observation matches well. However, when MODIS indicates snow in October and May, the model is underestimating SCA. Observed SCA data for the season 2004–2005 (Figure 4 top) indicate that the snow cover in the catchment was more or less constant (but with varying snow depths as shown in Figure 3 top), whereas for the season 2006–2007 (Figure 4 bottom) the observed SCA shows a great deal of dynamics in terms of snow melt and accumulation. This is due to the fact that the snow depths observed are much smaller than in the season 2004–2005, so complete

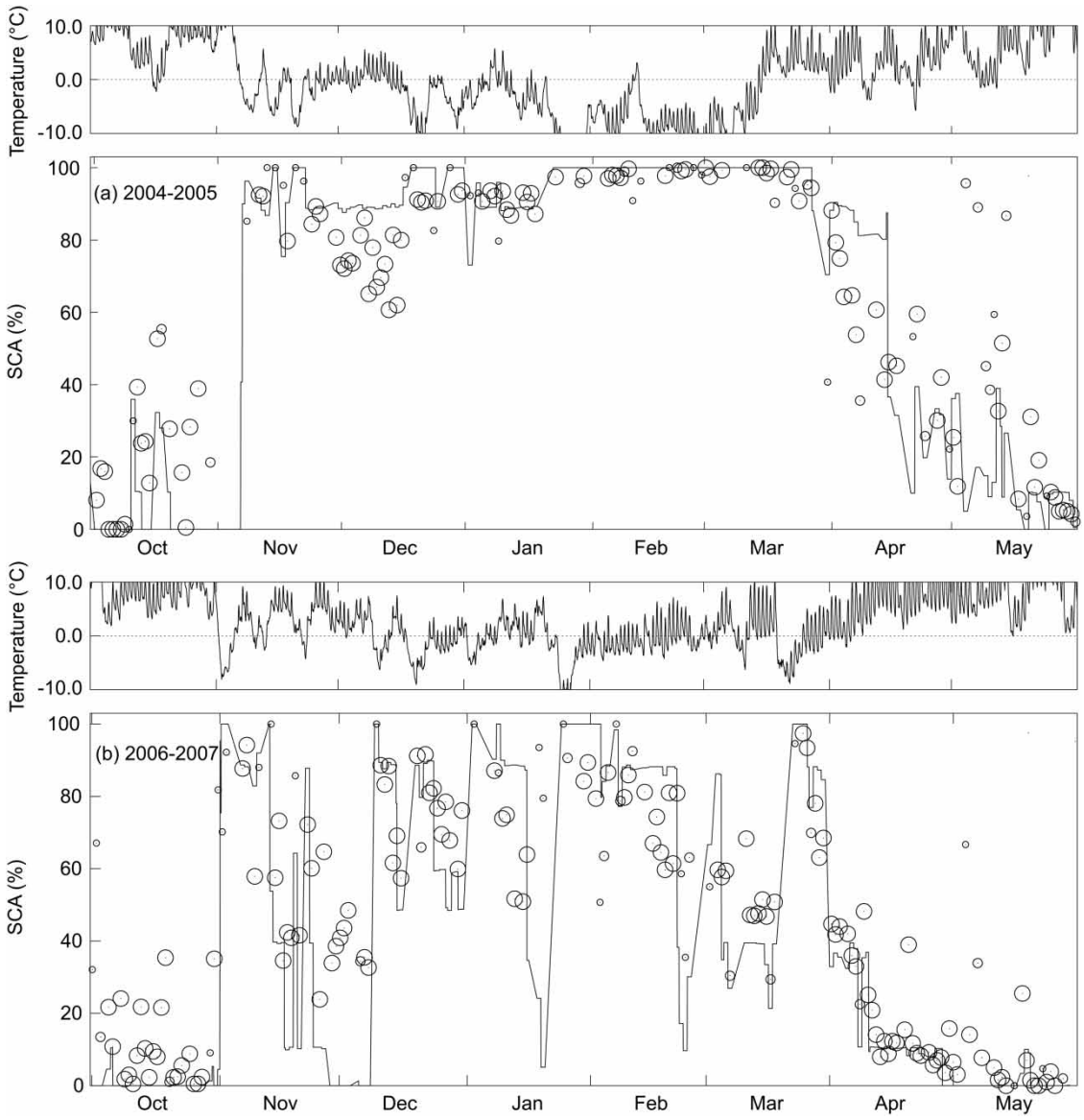

Figure 4 | Basin average snow covered area (SCA) for the Lammer catchment, 2004–2005 (top) and 2006–2007 (bottom). MODIS data are shown as circles, model results as solid lines. Size of circles indicates the cloud coverage over the catchment (large circles – cloud coverage less than 50%, medium circles – cloud coverage 50–80% and small circles cloud coverage 80–95%).

snow depletion is more likely to occur. The temporal evolution of the SCA from November to March is simulated well for both the winters shown.

Efficiency and errors for snow covered area

For SCA, the evaluation of the results is not straightforward as the model is based on elevation zones while the MODIS data are raster based. Additionally, the model simulates the amount (volume) of water stored in the form of snow, whereas MODIS snow cover data contain information only about the spatial extent of snow (i.e. whether a pixel is classified as snow, land or missing information). We used the method of Parajka & Blöschl (2008b) who compared MODIS snow cover data with SWE model simulations in an indirect way.

The comparison is performed in individual elevation zones of a catchment. Two types of snow error are evaluated. The first, termed model overestimation error (S_E^O), counts the number of days m_O when the hydrologic model simulates zone SWE greater than a threshold, but MODIS indicates that SCA less than a threshold is present in the zone, i.e.:

$$S_E^O = \frac{1}{m \cdot l} \sum_{j=1}^{l} m_O \wedge (\mathrm{SWE} > \xi_{\mathrm{SWE}}) \wedge (\mathrm{SCA} < \xi_{\mathrm{SCA}}) \quad (2)$$

where SWE is the simulated snow water equivalent in one zone, SCA is the MODIS snow covered area within this zone, m is the number of days where MODIS images are available (with cloud cover less than a threshold ξ_C (%)), l is the number of zones of a particular catchment, ξ_{SWE} (mm) is a threshold that determines when a zone can be essentially considered snow free in terms of the simulations and ξ_{SCA} (%) is a threshold that determines when a zone can be essentially considered snow free in terms of the MODIS data.

The second error, termed model underestimation error (S_E^U), counts the number of days m_U when the hydrologic model simulates snow less than a threshold in a zone but MODIS indicates that SCA greater than a threshold is present in the zone, i.e.:

$$S_E^U = \frac{1}{m \cdot l} \sum_{j=1}^{l} m_U \wedge (\mathrm{SWE} < \xi_{\mathrm{SWE}}) \wedge (\mathrm{SCA} > \xi_{\mathrm{SCA}}) \quad (3)$$

The percent or fraction of snow covered area, SCA, within each zone was calculated from the MODIS data as:

$$\mathrm{SCA} = \frac{S}{S + L} \quad (4)$$

where S and L represent the number of pixels mapped as snow and land, respectively, for a given day and a given zone. The reliability and accuracy of the SCA estimation depends on the spatial extent of clouds occurring in an elevation zone. Only those days of the SCA images were therefore used for a particular day and elevation zone if the cloud coverage, CC, was less than a threshold ξ_C:

$$\mathrm{CC} = \frac{C}{S + L + C} \quad (5)$$

where C represents the number of pixels mapped as cloud covered and CC is the fractional cloud cover for a particular day and elevation zone. The thresholds ξ_{SWE} (mm), ξ_{SCA} (%) and ξ_C (%) were chosen on the basis of a sensitivity analysis. The magnitude of the threshold ξ_C will affect the number of days for which MODIS images are available. Parajka & Blöschl (2008b) suggest a threshold of 60% of cloud coverage; Hall *et al.* (2010) used a threshold of 80% to develop the MODIS cloud-gap-filled snow map product. In this study, the whole range of cloud coverage is analysed. For 50% of the MODIS data, the cloud coverage was less than 50%, for 20% of the MODIS data cloud coverage was between 50 and 80% and for 30% of the MODIS data cloud coverage was larger than 80%. Three different ranges of cloud coverage are chosen: (1) CC < 50%, (2) 50% < CC < 80% and (3) CC > 80% over a catchment. The thresholds ξ_{SWE} and ξ_{SCA} are used to compare model simulations and MODIS snow cover observations to define the snow model errors.

RESULTS

Summary statistics of snow model performance and choice of thresholds

A sensitivity study was carried out to analyse the impact of different threshold values for ξ_{SWE} and ξ_{SCA} on Equations (2) and (3). Figure 5 shows the median overestimation (left) and underestimation (right) errors for a cloud coverage <50%. For clarity of presentation, the different cloud coverages are not shown. Overestimation errors decrease with increasing ξ_{SWE} but increase with increasing ξ_{SCA} (Figure 5 left); underestimation errors decrease with increasing ξ_{SCA} and increase with increasing ξ_{SWE} (Figure 5 right). The change in overestimation errors is smaller than the change in underestimation errors. The errors for SCA are less sensitive to the threshold ξ_{SWE} than to the threshold ξ_{SCA}. The largest median overestimation errors occur for small thresholds for SWE and large thresholds for SCA; the

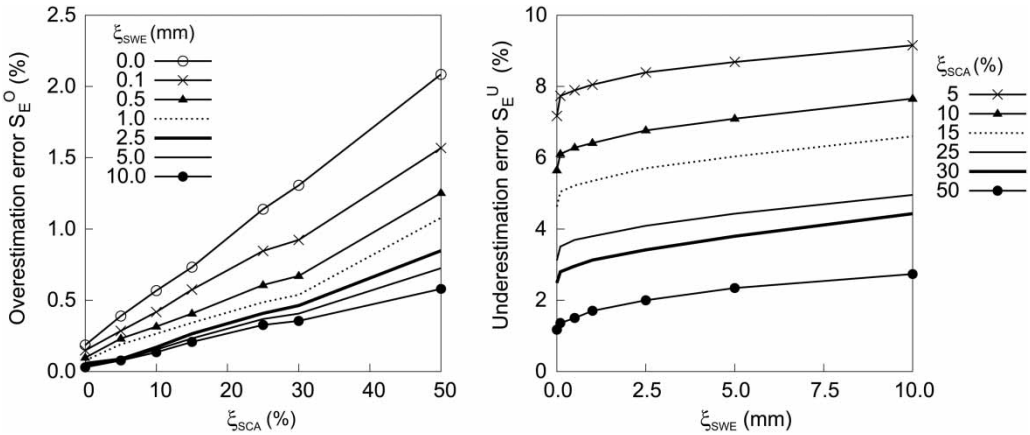

Figure 5 | Sensitivity analysis. Medians of snow overestimation errors (left) and snow underestimation errors (right) for cloud coverage <50%. Threshold values of $\xi_{SWE} = 2.5$ mm and $\xi_{SCA} = 30\%$ were chosen for further analyses.

largest underestimation errors occur for small thresholds for SCA and large thresholds for SWE. In order to achieve a compromise between over- and underestimation errors, we chose a threshold $\xi_{SWE} = 2.5$ mm as the median values and the percentile differences (P75%–P25%) for the overestimation errors are of the same order of magnitude for cloud coverage less than 80% (Figure 5 left). The threshold $\xi_{SCA} = 30\%$ was chosen as the overestimation errors increase only slightly from $\xi_{SCA} = 25$–30% compared to the increase of overestimation errors from $\xi_{SCA} = 30$–50% (Figure 5 left), and the underestimation errors are clearly smaller for $\xi_{SCA} = 30\%$ compared to $\xi_{SCA} = 25\%$ (Figure 5 right).

Table 2 summarises the overestimation errors for different thresholds ξ_{SWE} and different cloud coverage at a constant threshold $\xi_{SCA} = 30\%$. For cloud coverage less than 50%, the S_E^O overestimation errors are not very sensitive to the choice of the threshold ξ_{SWE}. The decrease of S_E^O with increasing threshold ξ_{SWE} is small. Median values range from 1.3% for a threshold $\xi_{SWE} = 0$ mm and 0.4% for a threshold $\xi_{SWE} = 10$ mm. The percentile difference (P75%–P25%) is stable around 0.6% which indicates that the shape of the cumulative distribution function (CDF) does not change much with changing thresholds. For a cloud coverage between 50 and 80%, the results are slightly more sensitive, with median overestimation errors ranging from 2.0% ($\xi_{SWE} = 0$ mm) to 0.5% ($\xi_{SWE} = 10$ mm). The percentile difference (P75%–P25%) is less stable from 0.8 to 2.0%. For a cloud extent of more than 80%, the errors are larger, with medians ranging from 3.3 to 1.0% for thresholds $\xi_{SWE} = 0$ mm and $\xi_{SWE} = 10$ mm, respectively. Percentile differences (P75%–P25%) are in the range of 0.9–2.2%. This shows that the choice of the thresholds ξ_{SWE} is getting more important as one moves up with the threshold forξ_C.

Table 2 | Statistical evaluation of the snow error overestimation CDFs for different ξ_{SWE} (mm) and constant $\xi_{SCA} = 30\%$. The first value is the median; the second value is the percentile difference (P75%–P25%) over 57 catchments for the period 2003–2009

ξ_{SWE} (mm)	CC <50%	50% < CC < 80%	CC >80%
0.0	1.3/0.8	2.0/2.0	3.3/2.2
0.1	0.9/0.6	1.6/1.6	2.6/1.9
0.5	0.7/0.6	1.4/0.9	2.2/1.3
1.0	0.5/0.6	1.2/1.1	1.8/1.4
2.5	0.5/0.6	0.8/0.9	1.5/1.2
5.0	0.4/0.7	0.7/0.8	1.2/1.0
10.0	0.4/0.6	0.5/0.8	1.0/0.9

Snow underestimation errors are evaluated for different thresholds of ξ_{SCA} but at a constant threshold $\xi_{SWE} = 2.5$ mm. Contrary to the overestimation errors, the underestimation errors S_E^U are more sensitive to the threshold ξ_{SCA} which was expected from the results in Figure 5. The S_E^U underestimation errors are largest for the restrictive threshold $\xi_{SCA} = 0$ (the graph for $\xi_{SCA} = 0$ is not shown in Figure 5, as the errors are too large). The errors decrease as the threshold gets less restrictive (increasing ξ_{SCA}), as one would expect. For example, for $\xi_{SCA} = 10\%$ and $\xi_{SWE} = 2.5$ mm (line with triangle

markers) the S_E^U errors are 6.8% for half the basins, for $\xi_{SCA} = 30\%$ and $\xi_{SWE} = 2.5$ mm (thick solid line) the S_E^U errors are 3.4%. The percentile difference (P75%–P25%) is not very stable and is larger than that of Parajka & Blöschl (2008b). In this study, for a threshold $\xi_{SCA} = 15\%$ the percentile difference is 3.8%, compared to 2.4% in Parajka & Blöschl (2008b) and for a threshold $\xi_{SCA} = 30\%$ the difference in this study is 3.0% compared to 1.1% in the above paper. However, they used slightly larger cloud coverage (50% vs. 60%), smaller catchments, especially in alpine areas, and fewer catchments in prealpine areas. Table 3 summarises the underestimation errors for tddifferent thresholds ξ_{SCA} and different cloud coverages. The results suggest that the use of a threshold of ξ_C is necessary, as the amount of information clearly decreases with the increase of cloud coverage.

Table 3 | Statistical evaluation of snow error underestimation errors for different ξ_{SCA} (%) and cloud coverage. $\xi_{SWE} = 2.5$ mm. The first value is the median; the second value is the percentile difference (P75%–P25%) over 57 catchments for the period 2003–2009

ξ_{SCA} (%)	CC <50%	50% < CC < 80%	CC >80%
0	12.5/7.5	19.5/11.2	14.1/9.6
5	8.4/5.3	15.5/9.9	13.1/8.7
10	6.8/4.4	13.1/8.7	12.5/7.4
15	5.7/3.8	10.7/7.0	11.5/6.8
25	4.1/3.2	7.2/5.8	9.5/5.7
30	3.4/3.0	6.4/5.5	8.9/5.0
50	2.0/1.6	3.1/3.3	5.9/3.8

Figure 6 shows the seasonal distribution of the median overestimation errors S_E^O and the median underestimation errors S_E^U for the thresholds $\xi_{SWE} = 2.5$ mm and $\xi_{SCA} = 30\%$. As expected, overestimation errors are small with the largest values in the range of 0.2% in the months February to April. Underestimation errors do have a clear seasonal cycle with peaks in March and April and October. For a SCA threshold $\xi_{SCA} = 30\%$ the largest error is around 0.8% in November. These results confirm Figure 4, where we showed an underestimation of snow by the model in the accumulation and depletion phases. With increasing cloud cover, the overestimation errors increase slightly whereas the increase in underestimation errors is more obvious. Interestingly, a threshold value $\xi_{SCA} = 30\%$ leads to underestimation errors in the summer months for cloud coverage larger than 50%. This indicates that some areas are marked as snow covered in MODIS whereas the model simulated no snow. Parajka & Blöschl (2006) found that the difference may be due to the cloud mask used in the snow mapping algorithm, where MODIS misclassified clouds as snow in summer months. Parajka *et al.* (2010) compared MODIS maps with grid maps of mean daily air temperatures in Austria and found a maximum of 1.4% of the pixels classified as snow in July and 3.2% of the pixels classified as snow in May when the mean air temperature was higher than 10 °C. We find similar values in prealpine regions in this study, with 1.6% of the pixels classified as snow in July and 5.8% of the pixels classified as snow in May.

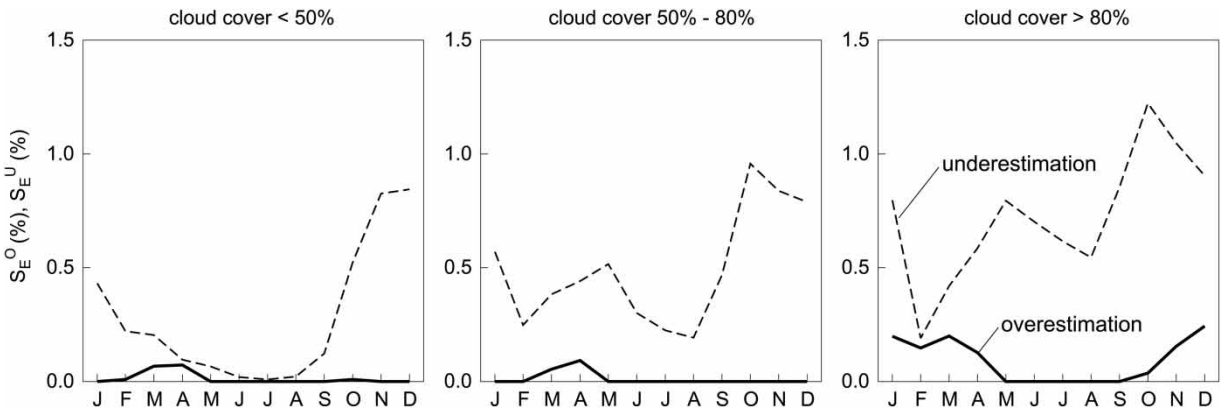

Figure 6 | Seasonal distribution of snow overestimation S_E^O (solid lines) and underestimation S_E^U (dashed lines) errors. Median values 2003–2009 for thresholds $\xi_{SWE} = 2.5$ mm and $\xi_{SCA} = 30\%$.

Further insight into the snow model results is provided by Figure 7. For each catchment, the overestimation errors S_E^O and underestimation errors S_E^U are analysed as a function of mean catchment elevation for the period 2003–2009. We show only the errors for the thresholds $\xi_{SWE} = 2.5$ mm and $\xi_{SCA} = 30\%$. Open circles indicate overestimation errors and dark circles indicate underestimation errors. For a cloud cover less than 50%, the overestimation errors are in the range of 0–2%, whereas the underestimation errors are larger with values ranging from 1 to 11%. With increasing cloud cover, the overestimation errors increase only slightly whereas the underestimation errors increase rapidly. Interestingly, the biggest differences between over- and underestimation errors can be observed for a mean catchment elevation smaller than 1,000 m a.s.l. For mean elevations larger than 1,000 m a.s.l., the difference is much smaller, indicating that the performance of the snow model is much better for higher altitudes. Zappa (2008) showed similar results in his study for Switzerland. There are several reasons for larger underestimation errors. First, the poorer performance of the snow model in the lower catchments can be attributed to the use of 500 m elevation zones. There are a number of catchments in prealpine areas with only one elevation zone, resulting in a SCA of either 0 (snow free) or 100% (snow covered), whereas in MODIS a more precise distinction of snow cover is possible. A second reason for the underestimation errors is misclassification of clouds as snow during summer months, as stated above. Another possibility for larger underestimation errors is that the majority of the errors occur during the melt periods. Therefore, areas that experience frequent melt during the winter may tend to have poorer performance statistics than areas that have a consistent snowpack for several months.

Spatial analysis of snow model performance

The spatial validation of the snow routine was carried out on a pixel by pixel basis. The threshold ξ_{SWE} is used for the distinction of snow cover in this analysis; a threshold for cloud cover ξ_C is not needed as only pixels that are not cloud covered in the MODIS data are accounted for; and the threshold ξ_{SCA} is not needed as the validation is carried out on the pixel scale and not on the catchment scale.

Figure 8 shows the spatial validation of the snow routine carried out on a pixel basis. As an example for a day with almost no cloud coverage, the extent of the snow cover is shown for February 3, 2008, according to MODIS data (top) and model results (bottom). No data and clouds are indicated by white areas, snow is shown as grey and snow free areas are shown as green. (The colour version of Figure 8 is available in the online version of the paper (http://www.iwaponline.com/nh/toc.htm).) MODIS data indicate that the mountainous regions are snow covered: the Alps are covered with snow with the exception of some valleys; also in the northern part of Austria the higher elevation pixels are snow covered. For determining snow cover from the model results, a threshold $\xi_{SWE} = 2.5$ mm was used. The results show a similar extent of the snow cover as the MODIS data: 81.5% of the

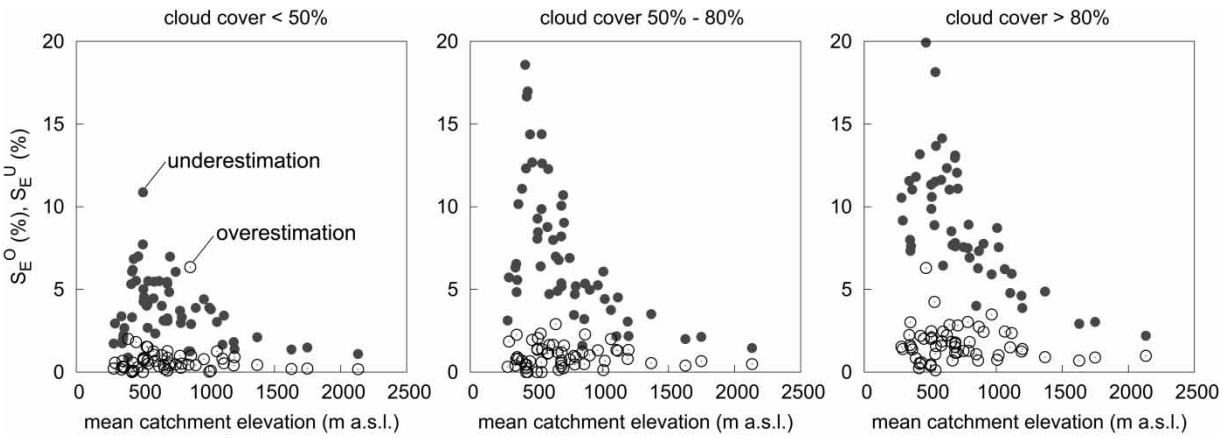

Figure 7 | Snow overestimation S_E^O (open circles) and underestimation S_E^U errors (dark circles) as a function of elevation. The period is 2003–2009, thresholds $\xi_{SWE} = 2.5$ mm and $\xi_{SCA} = 30\%$. Both snow overestimation and underestimation errors increase as the cloud coverage increases.

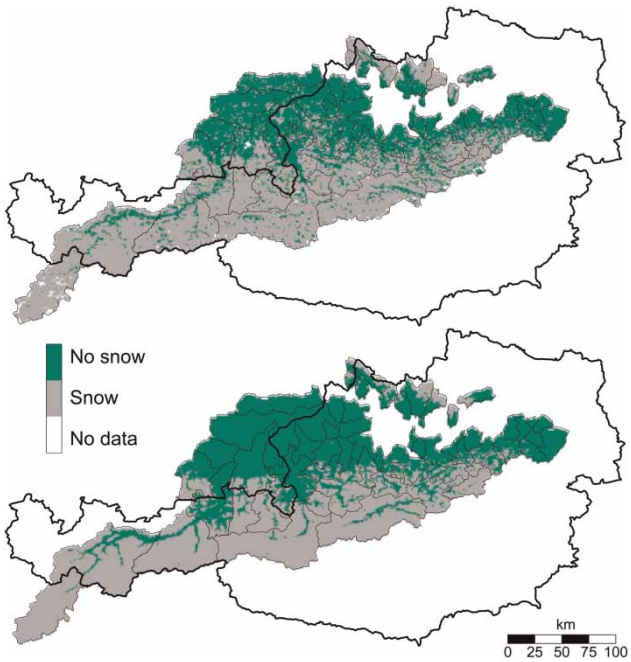

Figure 8 | Example pattern in the snow melt phase (3 February 2008). Top refers to MODIS data, bottom to model. White indicates cloud covered (no data available), green: snow free, grey: snow covered. Only model SWE larger than a threshold $\xi_{SWE} = 2.5$ mm were considered as snow. The colour version of this figure is available in the online version of the paper (http://www.iwaponline.com/nh/toc.htm).

pixels are correctly classified as snow covered and snow free, respectively, with alpine valleys and prealpine lowlands not covered by snow. 12.3% of the pixels are underestimated by the model, 4.7% of the pixels are overestimated by the model and 1.5% of the pixels do not contain data.

Figure 8 shows an example of a single day. To gain insight into the performance of the snow model for the entire evaluation period 2003–2009, we compared all available MODIS snow cover maps with the model results. We used two different measures. First, we compared the difference of days with simulated and observed snow cover on a pixel basis. Second, we calculated the hit rate H between MODIS and model results for snow covered days and snow free days.

For every pixel, the bias was calculated as

$$\text{bias} = \left(\frac{S_{\text{MODEL}}}{S_{\text{MODEL}} + L_{\text{MODEL}}} - \frac{S_{\text{MODIS}}}{S_{\text{MODIS}} + L_{\text{MODIS}}} \right) \times 100 \qquad (6)$$

where S_{MODEL} and L_{MODEL} refer to the number of days with snow cover and no snow, respectively, according to the model; and S_{MODIS} and L_{MODIS} refer to the number of days with snow cover and no snow, respectively, according to MODIS. Only days marked as cloud free in MODIS were considered. For the distinction of S_{MODEL} and L_{MODEL}, the threshold $\xi_{SWE} = 2.5$ mm was used. For simplicity, we used the terms positive bias when more days are snow covered in the model than MODIS and negative bias when fewer days are snow covered in the model than MODIS.

The spatial distribution of the bias (Figure 9) shows that in the prealpine parts MODIS indicates snow cover on more days than the model results whereas in alpine regions the model tends to indicate snow cover on more days than

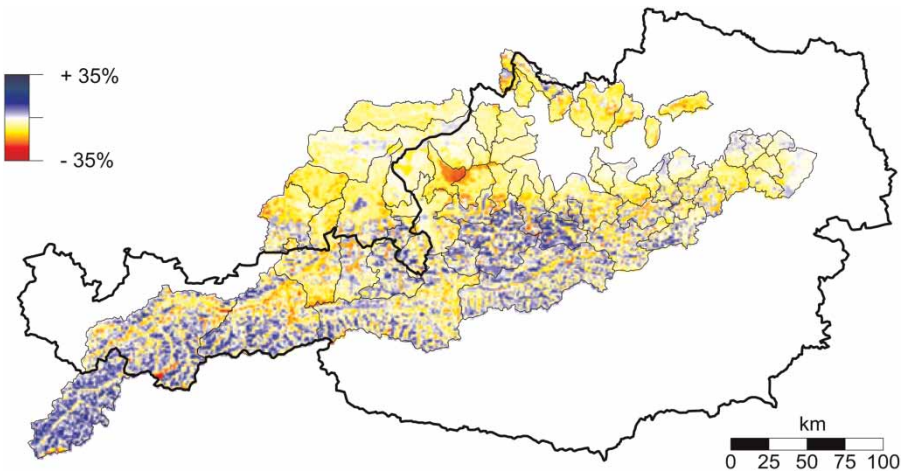

Figure 9 | Bias of the model results relative to MODIS data for the period 2003–2009. Red indicates negative bias (fewer days are snow covered in the model than MODIS), blue indicates positive bias. Only model SWE larger than 2.5 mm was considered as snow. The colour version of this figure is available in the online version of the paper (http://www.iwaponline.com/nh/toc.htm).

MODIS. On average, the negative bias is on the order of 15% of the cloud free days. The negative bias is even larger in parts of a prealpine catchment in the middle of the model area. There may be two reasons for this. First, the model structure for this catchment comprises a single elevation zone. Therefore, the temperature is assumed to be the same throughout the whole catchment, resulting in uniform SWE across the catchment. The topography, however, does vary by about 400 m within this catchment, so local differences in temperatures are possible. Second, the area underestimated by the model is covered by both coniferous and deciduous forests according to a land cover map (EEA, CORINE Land Cover 2000) which can cause problems in MODIS snow detection. For example, Simic *et al.* (2004) showed that MODIS products give realistic snow cover maps for an average of 93% of the days, with lower percentages for evergreen forests where MODIS has a tendency to overestimate snow. Hall *et al.* (2002) showed that MODIS has a tendency to underestimate snow in a forested area. The influence of land cover is analysed in more detail in Figure 10. Error CDFs with values derived from Figure 9 show hardly any difference for positive bias between forested and open land (left) whereas there is a clear difference for negative bias between forests and open land (right) with larger values for forests. This may be related to the model structure. We estimated parameters based on the land use and geology, but the use of a semi-distributed model requires mean parameters for each elevation zone. The use of a distributed model with hydrological response units could perhaps improve the snow model, but further analysis would be required to verify this.

Figure 11 shows the performance of the snow model for the winter seasons (October–May) of the years 2003–2009 for all cloud free days. The overall degree of agreement between MODIS and the model results is represented by the hit rate H (Wilks 1995):

$$H = \frac{a+d}{a+b+c+d} \tag{7}$$

with a, b, c, and d defined as in Table 4. Results show that the overall accuracy of the snow model is good with 98% of the model area having a hit rate H larger than 70% for the winter seasons of 2003–2009. Eighty-eight percent of the model area has a hit rate H larger 80 and 1.5% of the model area has have a hit rate H between 60 and 70%. The highest hit rates occur in the high elevations in the western part of Austria, which is not surprising as the snow model simulates snow in high elevations quite accurately and MODIS indicates snow cover in these areas. In the low parts of the model area, the hit rate H is also high (around 90%). This can be attributed to the fact that the model simulates no snow and the MODIS data confirm this. The medium elevation ranges show a smaller hit rate (around 70–80%), which is related to forest cover in these areas.

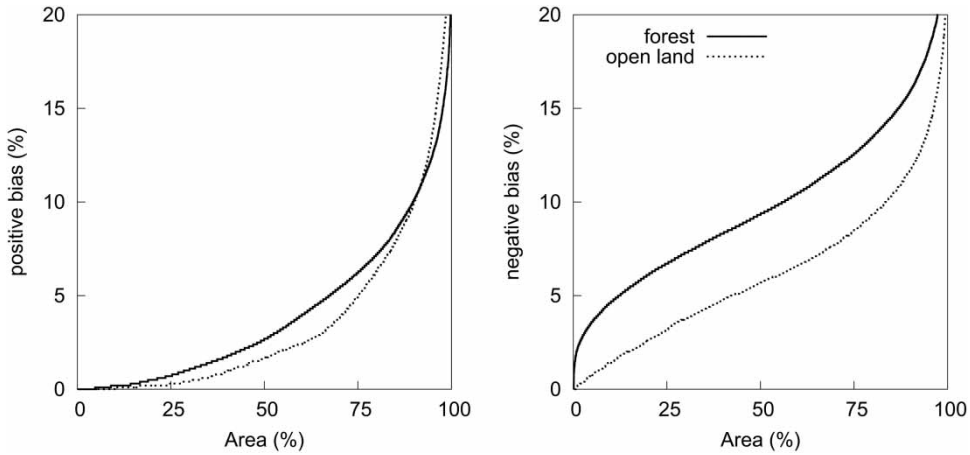

Figure 10 | CDFs of positive and negative biases (%) for forests and open land, pixel values. Land use taken from Corine. Threshold $\xi_{SWE} = 2.5$ mm.

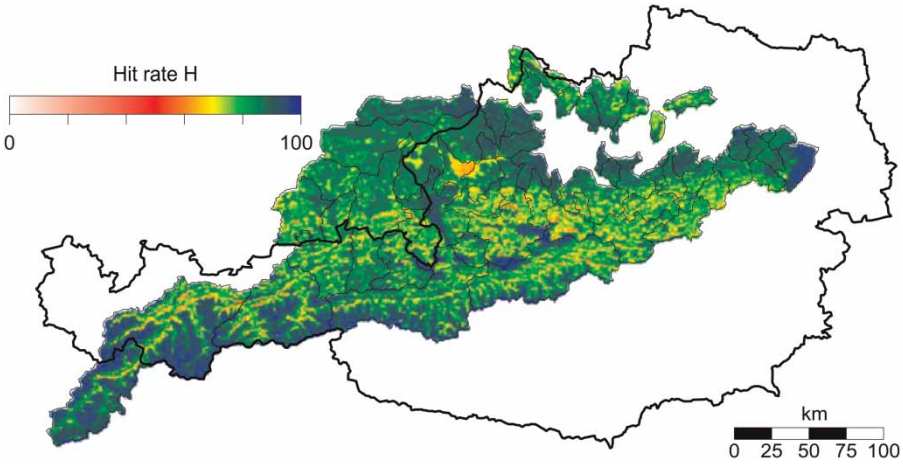

Figure 11 | Hit rate *H* of snow simulations for the winter season (October–May) in the period 2003–2009. Days with clouds are not considered. Threshold $\xi_{SWE} = 2.5$ mm. A colour version of this figure is available in the online version of the paper (http://www.iwaponline.com/nh/toc.htm).

Table 4 | Definitions for Eq. (7)

	MODIS snow	MODIS no snow
Model snow	a	b
Model no snow	c	d

DISCUSSION AND CONCLUSIONS

We have evaluated the snow model component of a conceptual semi-distributed hydrologic model run on an hourly time step. The model is used operationally for flood forecasting, but for this study we used it in a simulation mode with historical data. Parameters of the hydrologic model have been calibrated for 57 catchments manually in a three step routine. The annual water balance is approximated in a first step, seasonal patterns of streamflow were sought to be modelled correctly in a second step. The third step included the parameterisation of the fast flow components to correctly estimate the timing of the rising limbs and the peaks. This approach assured to account for different hydrological situations throughout the catchments.

A comparison of the temporal evolution of the SCA derived from MODIS data and SCA estimated from model results indicates good agreement between observed and simulated SCA values when cloud coverage is less than 80%. The timing of the snow accumulation and depletion periods is simulated well. However, discrepancies between model and MODIS are observed at the beginning and end of each snow season, but, as Klein & Barnett (2003) noted, 'This is perhaps not surprising as at these times, when snow would be expected to be thinnest and most patchy.'

We further evaluated the performance of the snow model using various error measures (Parajka & Blöschl 2008b). Simulated SWE and SCA estimated from a combination of MODIS (version 5) Terra and Aqua snow cover maps (Parajka & Blöschl 2008a) were compared for each day on the catchment scale. The selection of the cloud threshold ξ_C was found to be the most important factor for the evaluation of the snow model. Previous studies have used different thresholds for cloud coverage. For example, Şorman *et al.* (2009) used a threshold of 20% to calibrate a hydrologic model on streamflow and SCA data, Hall *et al.* (2010) used MODIS data with cloud coverage up to 80% for the development of a cloud-gap-filled MODIS daily snow cover product. Rodell & Houser (2004) used MODIS data when only 6% of the MODIS maps were cloud free. Results indicate that the errors are similar for $CC < 50\%$ and for $50\% < CC < 80\%$, but there are clear differences for $CC > 80\%$. Therefore, we propose to use a threshold value $\xi_C = 80\%$. The remaining threshold values were selected based upon a sensitivity study. It showed that results are less sensitive to the threshold for SWE than they are to the threshold for SCA. Based on the sensitivity study we selected threshold values $\xi_{SWE} = 2.5$ mm and $\xi_{SCA} = 30\%$ for the error analysis. We believe that the

chosen thresholds can be also used as in regions with similar physiographic characteristics. The value chosen for ξ_{SWE} is within the range of threshold values in the literature (i.e., Tong *et al.* 2009b; Roy *et al.* 2010); whereas the value chosen for ξ_{SCA} is slightly larger than the threshold used in Parajka & Blöschl (2008b). Results indicate that snow underestimation errors are larger than snow overestimation errors and that the thresholds have to be chosen with care as they have a large impact on the snow model efficiency. Interestingly, overestimation errors are not as sensitive to the threshold for cloud coverage ξ_C as are underestimation errors, and the seasonal error distribution shows that the model tends to underestimate snow in the summer months. This may be due to misclassification of clouds as snow in the MODIS data (Parajka & Blöschl 2006). Parajka *et al.* (2010) state, 'This misclassification occurs frequently, but tends to affect only a small area.' The error distribution as a function of elevation shows that larger underestimation errors occur in prealpine regions.

We also compared the spatial extent of simulated SCA and MODIS SCA data on a pixel basis taking into account only cloud free pixels. Generally, the snow model performance can be classified as good for the winter periods from 2003 to 2009. Eighty-eight percent of the model area is correctly classified as snow covered or snow free on more than 80% of the days. This value is similar to Strasser & Mauser (2001) who have shown an accuracy of 84% in their study in Northern Germany and Zappa (2008) who has shown an accuracy of 87% in a study in Switzerland. However, there are some discrepancies between simulated and observed SCA. The spatial evaluation indicates that at very high altitudes, the model tends to simulate snow on more days than what MODIS observes. This is in line with Koboltschnig *et al.* (2008). They attributed this to the fact that ridges and steep slopes at high altitudes are snow covered in the simulation whereas snow is expected to be blown away or redistributed by avalanches. In the transition zones from lowland to alpine areas, the model tends to underestimate the quantitiy of snow covered days. Two reasons may contribute to this; elevation changes not accounted for in the model structure; and underestimation of snow cover in forested areas. Analyses indicate that 500 m elevation zones may not be detailed enough to estimate SWE in the transition zones accurately. In this context Zappa (2008) noted that the disagreement in the transition zones may be due to uncertainties in observed precipitation, local and regional temperature gradients and in the model parameters. The underestimation of the remote sensing SCA in forested areas has already been shown in Simic *et al.* (2004) and the MODIS product summary page (MODIS 2010) states that 'the maximum expected errors are 15% for forests, 10% for mixed agriculture and forest, and 5% for other land covers'. The performance of the snow model in the transition zones could perhaps be improved using a spatially distributed model and a process based analysis of snow distribution patterns as proposed by Sturm & Wagner (2010). To confirm this, further analyses are required.

Overall, the comparison of simulated and observed SCA facilitated useful insights into the model performance as a function of space and time as well as other factors. Because of the usefulness in model evaluation, we would expect the snow cover data to be equally useful for data assimilation in a real time mode. This will be examined in future studies.

REFERENCES

Andreadis, K. & Lettenmaier, D. P. 2006 Assimilating remotely sensed snow observations into a macroscale hydrology model. *Adv. Water Res.* **29**, 872–886.

Bergström, S. 1976 Development and application of a conceptual runoff model for Scandinavian catchments. *Dept Water Resourc. Eng., Lund Inst. Technol./Univ. Lund, Bull. Ser.* **A52**, 134.

Blöschl, G. 2008 Flood warning – on the value of local information. *Int. J. River Basin Manage.* **6**, 41–50.

Blöschl, G. & Kirnbauer, R. 1992 An analysis of snow cover patterns in a small Alpine catchment. *Hydrol. Process.* **6**, 99–109.

Blöschl, G., Kirnbauer, R. & Gutknecht, D. 1991 Distributed snowmelt simulations in an Alpine catchment. 2. Parameter study and model predictions. *Water Resour. Res.* **27**, 3181–3188.

Blöschl, G., Kirnbauer, R., Jansa, J., Kraus, K., Kuschnig, D., Gutknecht, D. & Reszler, Ch. 2002 Using remote sensing methods for calibrating and verifying a spatially distributed snow model. *Österr. Wasser- und Abfallwirtschaft (ÖWW)* **54** (1/2), 1–16.

Blöschl, G., Reszler, C. & Komma, J. 2008 A spatially distributed flash flood forecasting model. *Environ. Model. Softw.* 2007, **23** (4), S. 2008, 464–478.

Braun, L. N. 1985 Simulation of Snowmelt-runoff in Lowland and Lower Alpine Regions in Switzerland. Dissertation. Zürcher Geographische Schriften, Heft 21. ETH, Zürich, Switzerland.

Déry, S. J., Salomonson, V. V., Stieglitz, M., Hall, D. K. & Appel, I. 2005 An approach to using snow areal depletion curves

inferred from MODIS and its application to land-surface modelling in Alaska. *Hydrol. Process.* **19**, 2755–2774.

DVWK 1996 *Ermittlung der Verdunstung von Land- und Wasserflächen*. DVWK-Merkblätter, Heft 238, Bonn, Germany.

EEA 2000 European Environmental Agency (EEA): CORINE Land Cover 2000. Available from: http://www.eea.europa.int.

Gafurov, A. & Bárdossy, A. 2009 Cloud removal methodology from MODIS snow cover product. *Hydrol. Earth Syst. Sci.* **13**, 1361–1373.

Garen, D. C. & Marks, D. 2005 Spatially distributed energy balance snowmelt modelling in a mountainous river basin: estimation of meteorological inputs and verification of model results. *J. Hydrol.* **315**, 126–153.

Haiden, T. & Pistotnik, G. 2009 Intensity-dependent parameterization of elevation effects in precipitation analysis. *Adv. Geosci.* **20**, 33–38.

Haiden, T., Kann, A., Stadlbacher, K., Steinheimer, M. & Wittmann, C. 2010 Integrated Nowcasting Through Comprehensive Analysis (INCA) - System Overview. ZAMG Report, 60p. Available from: http://www.zamg.ac.at/fix/INCA_system.doc (accessed 13 September 2010).

Hall, D. K. & Riggs, G. A. 2007 Accuracy assessment of the MODIS snow products. *Hydrol. Process.* **21**, 1534–1547.

Hall, D. K., Riggs, G. A., Salomonson, V. V., DiGirolamo, N. E. & Bayr, K. J. 2002 MODIS snow-cover products. *Remote Sens. Environ.* **83**, 181–194.

Hall, D. K., Riggs, G. A. & Salomonson, V. V. 2006 *MODIS/Terra Snow Cover Daily L3 Global 500 m Grid V005, January 2003 to December 2009*. National Snow and Ice Data Center, Boulder, Colorado, USA. Digital media, updated daily.

Hall, D. K., Riggs, G. A. & Salomonson, V. V. 2007 *MODIS/Aqua Snow Cover Daily L3 Global 500 m Grid V005, January 2003 to December 2009*. National Snow and Ice Data Center, Boulder, Colorado, USA. Digital media, updated daily.

Hall, D. K., Riggs, G. A., Foster, J. L. & Kumar, S. V. 2010 Development and evaluation of a cloud-gap-filled MODIS daily snow-cover product. *Remote Sens. Environ.* **114**, 496–503.

Immerzeel, W. W., Droogers, P., de Jong, S. M. & Bierkens, M. F. P. 2009 Large-scale monitoring of snow cover and runoff simulation in Himalayan river basins using remote sensing. *Remote Sens. Environ.* **113**, 40–49.

Kienzle, S. W. 2008 A new temperature based method to separate rain and snow. *Hydrol. Process.* **22**, 5067–2085.

Kirnbauer, R. & Schönlaub, H. 2006 Vorhersage für den Inn. *Wiener Mitteilungen* **199**, 69–84. In German.

Klein, A. G. & Barnett, A. C. 2003 Validation of daily MODIS snow cover maps of the Upper Rio Grande River Basin for the 2000–2001 snow year. *Remote Sens. Environ.* **86**, 162–176.

Koboltschnig, G. R., Schöner, W., Zappa, M., Kroisleitner, C. & Holzmann, H. 2008 Runoff modelling of the glacierized Alpine Upper Salzach basin (Austria): multi-criteria result validation. *Hydrol. Process.* **22**, 3950–3964.

Merz, R. & Blöschl, G. 2004 Regionalisation of catchment model parameters. *J. Hydrol.* **287**, 95–123.

Merz, R., Parajka, J. & Blöschl, G. 2009 Scale effects in conceptual hydrological modeling. *Water Resour. Res.* **45**, W09405.

MODIS 2010 MODIS web page information at: http://nsidc.org/data/docs/daac/modis_v5/mod10_l2_modis_terra_snow_cover_5min_swath.gd.html.

Nash, J. E. & Sutcliffe, J. V. 1970 River flow forecasting through conceptual models: Part I. A discussion of principles. *J. Hydrol.* **10**, 282–290.

Nester, T., Kirnbauer, R., Gutknecht, D. & Blöschl, G. 2011 Climate and catchment controls on the performance of regional flood simulations. *J. Hydrol.* **402**, 340–356, 2011.

Parajka, J. & Blöschl, G. 2006 Validation of MODIS snow cover images over Austria. *Hydrol. Earth Syst. Sci.* **10**, 679–689.

Parajka, J. & Blöschl, G. 2008a Spatio-temporal combination of MODIS images – potential for snow cover mapping. *Water Resour. Res.* **44**, W03406.

Parajka, J. & Blöschl, G. 2008b The value of MODIS snow cover data in validating and calibrating conceptual hydrologic models. *J. Hydrol.* **358**, 240–258.

Parajka, J. & Blöschl, G. 2012 MODIS-based Snow cover products, validation, and hydrologic applications. In: *Multiscale Hydrologic Remote Sensing: Perspectives and Applications* (N. B. Chang & Y. Hong, eds). CRC Press, Taylor & Francis Group, Boca Raton, FL, pp. 185–212.

Parajka, J., Merz, R. & Blöschl, G. 2003 Estimation of daily potential evapotranspiration for regional water balance modeling in Austria. In: *11th International Poster Day and Institute of Hydrology Open Day 'Transport of Water, Chemicals and Energy in the Soil – Crop Canopy – Atmosphere System'*, Slovak Academy of Sciences, Bratislava, pp. 299–306.

Parajka, J., Pepe, M., Rampini, A., Rossi, S. & Blöschl, G. 2010 A regional snow-line method for estimating snow cover from MODIS during cloud cover. *J. Hydrol.* **381**, 203–212.

Pu, Z., Xu, L. & Salomonson, G. A. 2007 MODIS/Terra observed seasonal variations of snow cover over the Tibetan Plateau. *Geophys. Res. Lett.* **34**, L06706, 6p.

Riggs, G. A., Hall, D. K. & Salomonson, V. V. 2006 MODIS Snow Products. User Guide to Collection 5. Available from: http://modis-snow-ice.gsfc.nasa.gov/sug_c5.pdf.

Rodell, M. & Houser, P. R. 2004 Updating a Land Surface Model with MODIS-Derived Snow Cover. *J. Hydrometeorol.* **5**, 1064–1075.

Roy, A., Royer, A. & Turcotte, R. 2010 Improvement of springtime streamflow simulations in a boreal environment by incorporating snow-covered area derived from remote sensing data. *J. Hydrol.* **390**, 35–44.

Schatzl, R. & Ruch, C. 2006 Internationales Hochwasserprognosemodell Mur. *Wiener Mitteilungen* **199**, 7–22. In German.

Schöber, J., Achleitner, S., Kirnbauer, R., Schöberl, F. & Schönlaub, H. 2010 Hydrological modelling of glacierized catchments focussing on the validation of simulated snow patterns – applications within the flood forecasting system of the Tyrolean river Inn. *Adv. Geosci.* **27**, 99–109.

Seibert, J. 1999 Regionalisation of parameters for a conceptual rainfall-runoff model. *Agric. For. Meteorol.* **98–99**, 279–293.

Simic, A., Fernandes, R., Brown, R., Romanov, P. & Park, W. 2004 Validation of VEGETATION, MODIS, and GOES + SSM/I snow-cover products over Canada based on surface snow depth observations. *Hydrol. Process.* **18**, 1089–1104.

Şorman, A. A., Şensoy, A., Tekeli, A. E., Şorman, A. Ü. & Akyürek, Z. 2009 Modelling and forecasting snowmelt runoff process using the HBV model in the eastern part of Turkey. *Hydrol. Process.* **23**, 1031–1040.

Steinheimer, M. & Haiden, T. 2007 Improved nowcasting of precipitation based on convective analysis fields. *Adv. Geosci.* **10**, 125–131.

Strasser, U. & Mauser, W. 2001 Modelling the spatial and temporal variations of the water balance for the Weser catchment 1965–1994. *J. Hydrol.* **254**, 199–214.

Sturm, M. & Wagner, A. M. 2010 Using repeated patterns in snow distribution modeling: an Arctic example. *Water Resour. Res.* **46**, W12549.

Sui, J. & Koehler, G. 2001 Rain-on-snow induced flood events in Southern Germany. *J. Hydrol.* **252**, 205–220.

Szolgay, J. 2004 Multilinear flood routing using variable travel-time discharge relationships on the Hron river. *J. Hydro. Hydromech.* **52**, 303–316.

Tekeli, A. E., Akyürek, Z., Şorman, A. A., Şensoy, A. & Şorman, A. Ü. 2005 Using MODIS snow cover maps in modeling snowmelt runoff process in the eastern part of Turkey. *Remote Sens. Environ.* **97**, 216–230.

Thirel, G., Salamon, P., Burek, P. & Kalas, M. 2011 Assimilation of MODIS snow cover area data in a distributed hydrological model. *Hydrol. Earth Syst. Sci. Discuss.* **8**, 1329–1364.

Tong, J., Déry, S. J. & Jackson, P. L. 2009a Topographic control of snow distribution in an alpine watershed of western Canada inferred from spatially-filtered MODIS snow products. *Hydrol. Earth Syst. Sci.* **13**, 319–326.

Tong, J., Déry, S. J. & Jackson, P. L. 2009b Interrelationships between MODIS/Terra remotely sensed snow cover and the hydrometeorology of the Quesnel River Basin, British Columbia, Canada. *Hydrol. Earth Syst. Sci.* **13**, 1439–1452.

Udnaes, H. C., Alfnes, E. & Andreassen, L. M. 2007 Improving runoff modelling using satellite-derived snow covered area? *Nord. Hydrol.* **38**, 21–32.

Wigmosta, M. S., Vail, L. W. & Lettenmaier, D. P. 1994 A distributed hydrology-vegetation model for complex terrain. *Water Resour. Res.* **30**, 1665–1679.

Wilks, D. S. 1995 Statistical methods in the atmospheric sciences. *Int. Geophys. Ser.* **59**, 238–240. Academic Press, San Diego.

Zappa, M. 2008 Objective quantitative spatial verification of distributed snow cover simulations – an experiment for the whole of Switzerland. *Hydrolog. Sci. J.* **53**, 179–191.

First received 10 February 2011; accepted in revised form 2 September 2011. Available online 23 May 2012